

ORIGINAL ARTICLE

OPEN

mARC1 in MASLD: Modulation of lipid accumulation in human hepatocytes and adipocytes

Amanda K. Jones¹ | Besnik Bajrami²  | Morgan K. Campbell¹ |
 Abdullah Mesut Erzurumluoglu³  | Qiusha Guo¹ | Hongxing Chen¹ |
 Xiaomei Zhang¹ | Svetlana Zeveleva¹ | David Kvaskoff² |
 Andreas-David Brunner² | Stefanie Muller³ | Vasudha Gathey¹ |
 Rajvee M. Dave¹ | James W. Tanner¹ | Sophia Rixen⁴ | Michel A. Struwe^{4,5} |
 Kathryn Phoenix⁶ | Kaitlyn J. Klumph¹ | Heather Robinson¹ | Daniel Veyel² |
 Annkatrin Muller² | Boris Noyvert³ | Boris Alexander Bartholdy³ |
 Agnes A. Steixner-Kumar³ | Jan Stutzki^{3,7} | Dmitriy Drichel^{3,7} |
 Steffen Omland^{3,7} | Ryan Sheehan⁸ | Jon Hill⁹ | Tom Bretschneider² |
 Dirk Gottschling¹⁰ | Axel J. Scheidig⁵ | Bernd Clement⁴ | Martin Giera^{2,11} |
 Zhihao Ding³ | John Broadwater¹ | Curtis R. Warren¹ 

¹Department of Cardiometabolic Disease Research, Boehringer Ingelheim Pharmaceuticals, Inc, Ridgefield, Connecticut, USA

²Department of Drug Discovery Sciences, Discovery Science Technologies, Boehringer Ingelheim Pharma GmbH & Co., Biberach an der Riss, Germany

³Department of Global Computational Biology and Digital Sciences, Boehringer Ingelheim Pharma GmbH & Co., Biberach an der Riss, Germany

⁴Department of Pharmacy, Pharmaceutical Institute, Christian Albrechts University, Kiel, Germany

⁵Department of Biology, Institute of Zoology-Structural Biology, Christian Albrechts University, Kiel, Germany

⁶Department of Biotherapeutics Discovery, Boehringer Ingelheim Pharmaceuticals, Inc, Ridgefield, Connecticut, USA

⁷Data Science Chapter, BI X GmbH, Ingelheim am Rhein, Germany

⁸Department of Immunology and Respiratory Disease Research, Boehringer Ingelheim Pharmaceuticals, Inc, Ridgefield, Connecticut, USA

⁹Department of Global Computational Biology and Digital Sciences, Boehringer Ingelheim Pharmaceuticals, Inc, Ridgefield, Connecticut, USA

¹⁰Department of Medicinal Chemistry, Boehringer Ingelheim Pharma GmbH & Co., Biberach an der Riss, Germany

¹¹The Center for Proteomics and Metabolomics, Leiden University Medical Center, Leiden, the Netherlands

Correspondence

Curtis R. Warren, Department of
 Cardiometabolic Disease Research, Boehringer
 Ingelheim Pharmaceuticals, Inc., 900 Ridgebury
 Rd, Ridgefield, CT 06877, USA.
 Email: curtis.warren@boehringer-ingelheim.com
[com](http://www.com)

Abstract

Background: Mutations in the gene MTARC1 (mitochondrial amidoxime-reducing component 1) protect carriers from metabolic dysfunction-associated steatohepatitis (MASH) and cirrhosis. MTARC1 encodes the

Abbreviations: GalNAc-siRNA, N-acetylgalactosamine-conjugated short-interfering RNA; GWAS, genome-wide associations study; KO, knockout; mARC1/MTARC1, mitochondrial amidoxime-reducing component 1; MASLD, metabolic dysfunction-associated steatotic liver disease; MASH, metabolic dysfunction-associated steatohepatitis; MR, Mendelian randomization; PHH, Primary human hepatocytes; SVF, stromal vascular fraction of adipose tissue.

Amanda K. Jones and Besnik Bajrami contributed equally.

Supplemental Digital Content is available for this article. Direct URL citations are provided in the HTML and PDF versions of this article on the journal's website, www.hepcommjournal.com.

This is an open access article distributed under the terms of the Creative Commons Attribution-Non Commercial-No Derivatives License 4.0 (CCBY-NC-ND), where it is permissible to download and share the work provided it is properly cited. The work cannot be changed in any way or used commercially without permission from the journal.

Copyright © 2024 The Author(s). Published by Wolters Kluwer Health, Inc. on behalf of the American Association for the Study of Liver Diseases.

mARC1 enzyme, which is localized to the mitochondria and has no known MASH-relevant molecular function. Our studies aimed to expand on the published human genetic mARC1 data and to observe the molecular effects of mARC1 modulation in preclinical MASH models.

Methods and Results: We identified a novel human structural variant deletion in MTARC1, which is associated with various biomarkers of liver health, including alanine aminotransferase levels. Phenome-wide Mendelian Randomization analyses additionally identified novel putatively causal associations between MTARC1 expression, and esophageal varices and cardio-respiratory traits. We observed that protective MTARC1 variants decreased protein accumulation in in vitro overexpression systems and used genetic tools to study mARC1 depletion in relevant human and mouse systems. Hepatocyte mARC1 knockdown in murine MASH models reduced body weight, liver steatosis, oxidative stress, cell death, and fibrogenesis markers. mARC1 siRNA treatment and overexpression modulated lipid accumulation and cell death consistently in primary human hepatocytes, hepatocyte cell lines, and primary human adipocytes. mARC1 depletion affected the accumulation of distinct lipid species and the expression of inflammatory and mitochondrial pathway genes/proteins in both in vitro and in vivo models.

Conclusions: Depleting hepatocyte mARC1 improved metabolic dysfunction–associated steatotic liver disease–related outcomes. Given the functional role of mARC1 in human adipocyte lipid accumulation, systemic targeting of mARC1 should be considered when designing mARC1 therapies. Our data point to plasma lipid biomarkers predictive of mARC1 abundance, such as Ceramide 22:1. We propose future areas of study to describe the precise molecular function of mARC1, including lipid trafficking and subcellular location within or around the mitochondria and endoplasmic reticulum.

INTRODUCTION

Metabolic dysfunction–associated steatotic liver disease (MASLD; previously NAFLD) and the advanced form, metabolic dysfunction–associated steatohepatitis (MASH; previously NASH) are chronic polygenic liver diseases associated with metabolic syndrome.^[1] Up to 10% of patients with MASH will progress to cirrhosis with a risk for HCC and death from liver decompensation.^[2] Currently, there are no approved therapies for the treatment of MASH, and the high global incidence of MASH represents a significant unmet medical need.^[3] Hepatocytes, hepatic stellate cells, and immune cells such as Kupffer cells and monocyte-derived macrophages have been the primary focus in MASH therapeutic concepts. MASH is promoted by systemic dysmetabolism, through a variety of mechanisms including tissue crosstalk between the adipose tissue and liver.^[4–7]

Several human genes with potential causal relationships to MASH phenotypes have been discovered through population genetics approaches, including the mitochondrial amidoxime–reducing component 1 gene (*MTARC1*, encoding outer mitochondrial membrane protein mARC1).^[8–13] Missense and nonsense variants in *MTARC1* were identified in a genome-wide association study (GWAS), which implicated these variants in protecting their carriers from MASH phenotypes, including reduced risk for MASH, hepatic steatosis, liver enzyme elevations, cirrhosis, and all-cause liver-related mortality.^[9,12]

mARC1's enzymatic activity was first observed in rat liver lysates in the 1960s.^[14] It was later described in porcine liver mitochondrial preparations as a molybdenum cofactor-dependent enzyme capable of reducing xenobiotics and certain endogenous *N*-hydroxylated compounds in concert with the cytochrome B5 electron transfer proteins and NADH.^[14] Despite the long-standing knowledge of mARC1's enzymatic functions, mechanistic

studies defining the role of mARC1 enzyme as it relates to metabolic diseases or liver biology are limited.

In this manuscript, we present genetic data complementing the published associations of *MTARC1* with phenotypes related to MASLD and cirrhosis and functional characterization of the protective genetic variants. In addition, we utilized long-read sequencing to identify a novel structural variant deletion in *MTARC1* and analyzed its association with various liver health-related traits. We also carried out phenome-wide Mendelian Randomization (MR) analyses to identify potential repurposing opportunities. Finally, we report data from preclinical experiments that build on the body of literature testing the potential utility of mARC1-targeted therapies for MASLD^[15] by extending the study of mARC1's function into human adipocytes. The multiomics analyses employed in these systems serve as a molecular spotlight revealing the physiological effects of mARC1's function in MASH.

METHODS

Ethics statement

All animal procedures were approved by the Institutional Animal Care and Use Committee of Boehringer Ingelheim Pharmaceuticals or Gubra Aps. Both research locations are accredited by the Association for Assessment and Accreditation of Laboratory Animal Care (AAALAC) and work performed at Gubra Aps was licensed by the Danish Animal Experimentation Council. All animal procedures are reported according to the Animal Research: Reporting of In Vivo Experiments (ARRIVE) guidelines.^[16]

All cell lines, primary human cells, and human tissues were obtained from commercial vendors in accordance with internal compliance protocols. All primary cells and human tissues were deidentified and no whole-genome sequencing data were produced. Most of the in silico research has been conducted using the UK Biobank Resource under Application Number 57952.

Animal husbandry

All animals were housed on a 12:12 hour light-dark cycle with all compound treatments and tissue collection occurring during the light cycle. Animals were group-housed except for studies performed at Gubra Aps where mice were individually housed for the duration of experiments. Animals had ad-lib access to food and water and were housed with bedding, shelters, and nesting supplies or chewing sticks for enrichment. A summary of the mouse strains and diets used across studies and 2 experimental locations used in this

manuscript can be found in Supplemental Methods, Tables S6 and S7, <http://links.lww.com/HC9/A798>.

Cloning—Variant plasmids, Overexpression plasmids

Cloning and purification of expression plasmids, lentivirus transfer plasmids, and lentivirus packaging plasmids was performed at Genscript, New Jersey, USA. *MTARC1* coding sequence was downloaded from NCBI, transcript ID NM_022746.4.

Data analysis

All data were analyzed using GraphPad Prism Version. Pairwise comparisons were performed using Student *t* test. For the comparison of the 3 groups, one-way ANOVA was performed. For groups of 4 or more groups, a *t* test was first performed to compare control and diseased conditions, then one-way ANOVA with Dunnett's comparison was performed to compare treatment groups to the diseased group. Longitudinal data were analyzed by two-way ANOVA with repeated measures and pairwise comparisons analyzed within a given time point. Data are presented as mean \pm SEM with individual data points represented in bar graphs. Significance is considered at $p < 0.05$.

The detailed methodology can be found in the Supplemental Methods, <http://links.lww.com/HC9/A798> and Supplemental Tables, <http://links.lww.com/HC9/A799>.

RESULTS

Variants affecting *MTARC1* function and/or expression are putatively causally associated with liver enzyme levels and liver disease progression

We replicated the previously published associations between nonsynonymous variants in *MTARC1* and protection from MASH, cirrhosis, liver-related mortality, and other MASLD-associated phenotypes utilizing a GWAS approach in ~500,000 UK Biobank participants (Supplemental Data Tables 1–3, <http://links.lww.com/HC9/A799>). The protective effects of 2 variants (ie, rs12023067 and rs2642438) on circulating alanine aminotransferase levels were sex-specific and/or sex-dependent (Supplemental Genetics Figure S1, <http://links.lww.com/HC9/A800>). In addition, our phenome-wide MR analyses identified a putatively causal link between mARC1 expression levels and the risk of esophageal varices (Supplemental Data Tables S3–S6, <http://links.lww.com/HC9/A799>, Supplemental Genetics Figure S2, <http://links.lww.com/HC9/A800>).^[17] Utilizing long-read

sequencing technologies to call structural variants in the human genome and imputation into UK Biobank, we also identified a common 64-base structural variant deletion overlapping with the 3'UTR of *MTARC1*, which is significantly associated with circulating alanine aminotransferase, HDL cholesterol, triglycerides, and albumin levels (Figure 1A, Supplemental Data Table S7, <http://links.lww.com/HC9/A799>).

Previous studies indicated that the protective loss-of-function *MTARC1* variants identified by genetics do not affect enzymatic activity or protein folding.^[18,19] We reasoned that the protective effect of these variants must be mediated by some other mechanism such as protein stability or subcellular localization. Consequently, we studied the localization and protein accumulation of 3 published human missense and nonsense variants associated with protection from MASH (A allele of rs2642438, p.M187K, and p.R200*),^[11] as well as one synthetic mutation known to abrogate the enzymatic function of the protein, p.C273A^[20] using in vitro overexpression experiments.

We identified several cell lines that were positive for mARC1 including the hepatoma cell lines HepG2 and HuH7,^[21] as well as HEK293T,^[22] and several cell lines that were negative for mARC1, including the glioblastoma cell line U-138MG (Supplemental Figure S1A, <http://links.lww.com/HC9/A801>).^[23] We made stable cell lines in the U-138MG background expressing each variant of *MTARC1*. In these stable cell lines, there was less accumulation of the variant proteins compared with the protein encoded by the major risk allele of *MTARC1* (Figure 1C). The truncation variant p.R200* was not detectable by western blot. To rule out differences in mRNA abundance in explaining differential protein accumulation of the variant proteins, we normalized the western blot data to mRNA abundance, and the effect of mARC1 variants to reduce protein abundance was sustained (Figure 1C, Supplemental Figure S1B, <http://links.lww.com/HC9/A801>). Transient transfection experiments of *MTARC1* variants were repeated in HEK293T cells and resulted in the same rank-order of protein accumulation that was observed in the stable U-138MG cell lines (Supplemental Figure S1C, <http://links.lww.com/HC9/A801>).

Next, we used the mARC1-negative U-138MG cell line for localizing variant mARC1 proteins within the cell using confocal microscopy and transient transfections with a construct expressing c-terminally MYC-tagged mARC1 variants. Although our western blotting experiments indicated that the variant transcripts produce less protein, we were able to identify cells that expressed each variant protein including the nonsense variant p.R200*. All mARC1 variants colocalized with TOMM20, an outer mitochondrial membrane marker (Figure 1D).

MTARC1 protective variants do not affect enzyme activity, folding, or active site architecture of the mARC1 protein^[18,19] but do affect protein accumulation

(Figure 1). As such, protein depletion is a reasonable approach to phenocopy the genetic variants in patients. To support our experimental designs related to protein depletion in cellular and in vivo MASH models, we quantified the half-life of the mARC1 protein in HepG2 cells to be 60 hours^[24] (Supplemental Figure S1D, <http://links.lww.com/HC9/A801>).

Pleiotropic effects of variants affecting *MTARC1* function and/or expression on heart and respiratory disease risk

To identify novel putatively causal effects of *MTARC1* expression on susceptibility to heart and respiratory diseases, we carried out *cis*-expression quantitative trait locus-based phenome-wide MR analyses followed by fine mapping^[25] and colocalization ("MR+Coloc", henceforth; see Methods). We identified strong MR+Coloc evidence (Lowest MR *p* value = 1.9×10^{-8} ; Coloc $H4 \approx 99\%$) linking *MTARC1* expression levels in lung disease-relevant tissues to FEV₁—a clinically relevant lung function measure (Supplemental Genetics Figure S3, <http://links.lww.com/HC9/A800>). Complementing this potential link to respiratory disease risk, we identified MR+Coloc evidence linking *MTARC1* expression to lymphangioleiomyomatosis (Supplemental Genetics Figure S4, <http://links.lww.com/HC9/A800>), a rare and progressive interstitial lung disease.

In line with *MTARC1*'s suspected links to heart disease, we identified strong MR+Coloc evidence linking increased *MTARC1* expression levels to myocardial infarction risk, blood pressure, and irbesartan and ezetimibe usage—medications used to treat high blood pressure and LDL cholesterol, respectively (Supplemental Genetics Figures S5–S7, <http://links.lww.com/HC9/A800>). In addition, there is also weaker but complementary evidence from MR+Coloc linking increased *MTARC1* expression to atrial fibrillation risk, angina pectoris, gamma-glutamyl-leucine levels, and insulin sensitivity (Supplemental Genetics Figures S8–S10, <http://links.lww.com/HC9/A800>). Full results (incl. > 700k analyses) are available in Supplemental Data Table S6, <http://links.lww.com/HC9/A799>, for further hypothesis generation or hypothesis-driven analyses related to *MTARC1*.

Tissue expression profile and subcellular localization of mARC1 in human and preclinical species

Using a publicly accessible data set (genotype-tissue expression),^[26] we confirmed hepatic *MTARC1* expression (mean transcripts per million reads 9.3) and observed that the transcript is most abundant in human adipose tissue (Figure 2A, average transcripts per

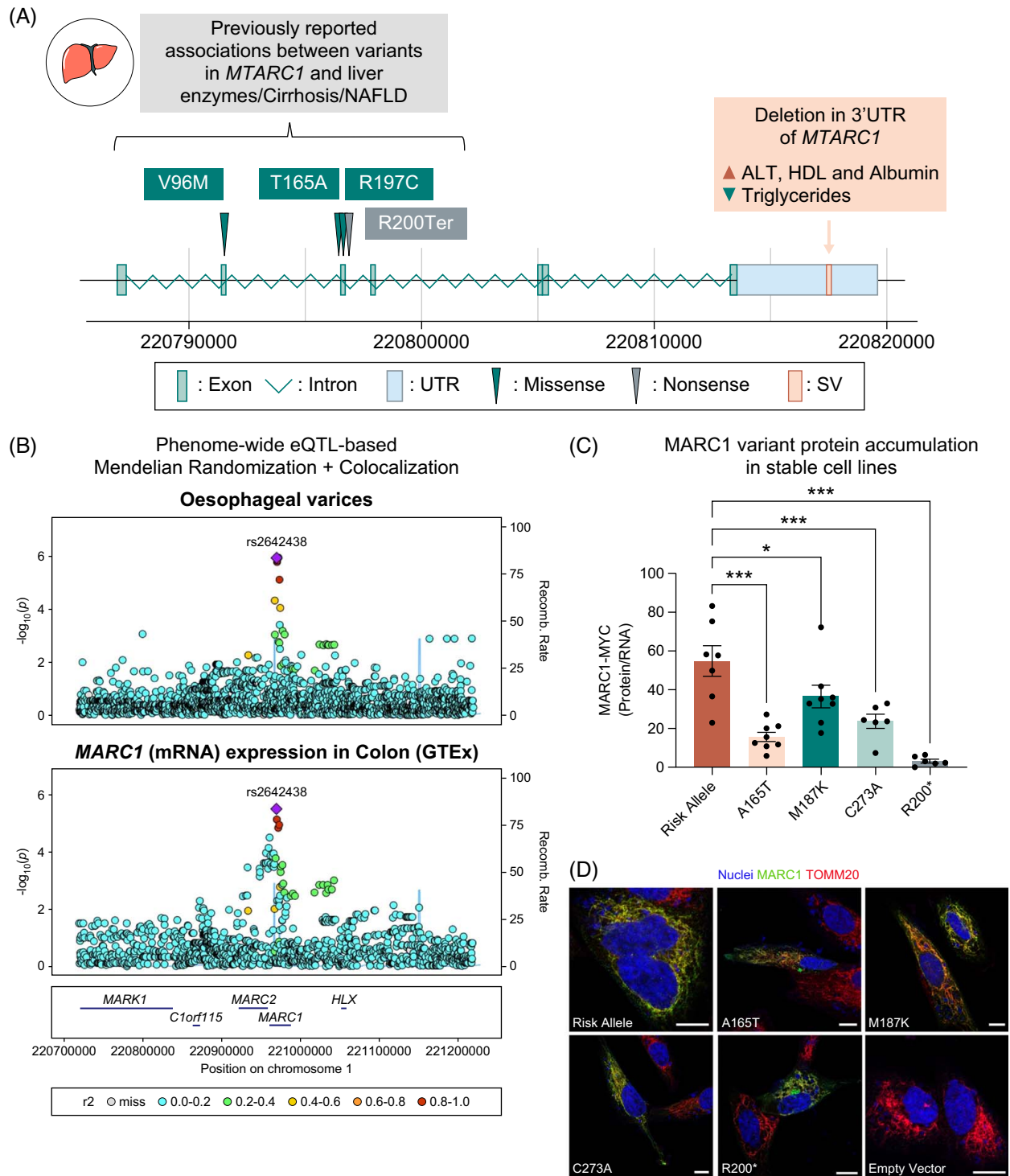


FIGURE 1 Genetic variants in *MTARC1* are associated with liver enzyme levels and susceptibility to and progression of MASLD-related and cirrhosis-related human traits—likely by decreasing mARC1 protein accumulation. (A) Schema of previously reported associations between variants in *MTARC1* (including the novel SV-deletion identified in this study) and liver enzymes and liver disease-related outcomes. (B) Phenome-wide Mendelian randomization analyses followed by colocalization analyses identified putatively causal links between *mARC1* expression levels and susceptibility to develop esophageal varices (IEU OpenGWAS study ID: finn-b-I9_VARICVEOES).^[38] (C) mARC1 protein expression in U-138 MG-derived stable cell clones transfected with vectors encoding variants of *MTARC1*. Risk allele: A allele of rs2642438 (coding for missense: p.T165A), Protective alleles: G allele of rs2642438, p.M187K, and p.R200*; Synthetic: p.C273A. Western blot quantitation is normalized to mRNA expression. Data are presented as means \pm SEM, $n = 6-8$ clones/variant. (D) Immunofluorescence imaging of human U-138 MG cells expressing mARC1 variant proteins (green), TOMM20 (mitochondria—red), nuclei (blue) labeled. Scale bars, 10 μ m. * $p \leq 0.05$, *** $p \leq 0.001$, one-way ANOVA. Abbreviations: ALT, alanine aminotransferase; eQTL, expression quantitative trait locus; GWAS, genome-wide association study; MASLD, metabolic dysfunction-associated steatotic liver disease; *MTARC1*, mitochondrial amidoxime-reducing component 1; SV, structural variant.

million reads value 37). We measured the expression of mARC1 in human liver and adipose tissue using western blotting and quantitative reverse transcription PCR and confirmed that *MTARC1* mRNA is more abundant in the adipose than in the liver of humans (Figure 2A). This difference in mRNA abundance did not translate to protein in our western blot analyses; mARC1 protein abundance was equivalent in human liver and adipose tissues (Figure 2A).

We employed multiplexed immunofluorescence histology of human liver sections to determine the hepatic cell types expressing the mARC1 protein. mARC1 expression was confirmed in human hepatocytes and in cluster of differentiation 68 (CD68)-positive cells (macrophages, Figure 2B). *MTARC1* expression was also observed in CD14⁺ (cluster of differentiation 14) monocytes in a published^[27] single-cell RNAseq data set of peripheral blood mononuclear cells from patients with cirrhosis. *MTARC1* was most highly expressed in a subpopulation of MHCII-low/SELL⁺ cells (average log fold-change = 0.24, $p < 1.5 \times 10^{-25}$) and expressed lowest in an MHCII-high subpopulation (Supplemental Figure S2A, <http://links.lww.com/HC9/A802>). Despite this evidence for *MTARC1* expression in myeloid cells in vivo, we were unable to confirm mARC1 protein expression in primary human Kupffer cells, monocytes, or monocyte-derived macrophages in culture (Supplemental Figures S2B, S2C, <http://links.lww.com/HC9/A802>). We observed mARC1 protein expression in the human monocyte cell line THP-1, but only at passage zero, and thus we could not pursue functional studies of mARC1 in myeloid cells in vitro.

In mice, mARC1 mRNA and protein abundance were greatest in the liver with low mRNA abundance detected in white (inguinal, gonadal, and perirenal) and brown adipose depots (Figure 2C). In mouse liver *Mtarc1* expression was confirmed in hepatocytes by colocalization with ASGR1 but not F4/80⁺ cells (representing macrophages) (Figure 2C).

We observed the localization of exogenous mARC1 using super-resolution microscopy in a human hepatoma cell line-derived mARC1 knockout (KO) cell line (Supplemental Figure S2E, <http://links.lww.com/HC9/A802>). Localizations of exogenous epitope-tagged mARC1 were distributed on the outer edge of the mitochondria defined by the mitochondrial matrix marker HSP60 (Figure 2D), which supports the published localization of mARC1 to the outer mitochondrial membrane.^[28]

mARC1 expression promotes steatosis, oxidative stress, and cell death in hepatocytes in vitro

To validate mARC1 as a therapeutic target for MASH, we first studied the functional effects of mARC1 depletion and overexpression in human in vitro

hepatocyte models, focusing on functional outcomes related to hepatoprotection. The half-life of mARC1 in vitro is incompatible with knockdown studies in traditional short-lived primary human hepatocyte (PHH) culture systems. To circumvent this obstacle, PHH spheroids and a long-term two-dimensional PHH culture system were used with *N*-acetylgalactosamine-conjugated short-interfering RNA (GalNAc-siRNA) tools to deplete mARC1 mRNA and protein. The potency and durability of the GalNAc-si*MTARC1* knockdown effects were characterized in time course and dose-response studies (Figure 3A, Supplemental Figure S3A, <http://links.lww.com/HC9/A803>). We observed maximal mARC1 protein knockdown (65%) 10 days after GalNAc-siRNA treatment. mRNA knockdown reached 90% as early as 3 days after GalNAc-siRNA treatment and persisted for up to 14 days in culture.

To validate human genetic findings associating *MTARC1* loss-of-function alleles with protection from MASLD,^[11] we knocked down *MTARC1* in PHHs using a long-term 2-dimensional culture system and studied steatosis using high-content microscopy. GalNAc-si*MTARC1* reduced lipid accumulation under both baseline conditions (in the absence of exogenous fatty acids) and in the presence of increasing doses of palmitate (Figure 3B). These studies were replicated in a HEK293T-derived *MTARC1*-KO cell line (Supplemental Figure S3B, S3C, <http://links.lww.com/HC9/A803>). In this cell line, lipid reductions during palmitate treatment were not statistically significant, but the observed effects had the same directional trend. GalNAc-si*MTARC1* treatment reduced the abundance of oxidized glutathione, a marker of oxidative stress, in PHH spheroids (Figure 3C).

We hypothesized that mARC1 promotes the onset and progression of MASH in humans by increasing hepatocyte stress and death through a metabolic mechanism. To test this hypothesis, we reconstituted mARC1 in *MTARC1*-KO hepatoma cell lines by transducing them with lentiviruses encoding the *MTARC1* risk allele or the *MTARC1* protective allele (the nonsense variant p.R200*). Overexpression of the risk allele resulted in a 15%–25% decrease in mitochondrial oxygen consumption (Figure 3D, Supplemental Figure S3D, <http://links.lww.com/HC9/A803>). Using microscopy-based methods in combination with overnutrition conditions relevant to human MASH (fatty acids, carbohydrates, and insulin), we observed that the overexpression of the *MTARC1* risk allele promoted mitochondrial dysfunction and cell death as quantified by reduced mitochondrial membrane potential, membrane permeability, and annexin V reactivity (Figure 3E, Supplemental Figure S3E, <http://links.lww.com/HC9/A803>). To further profile these KO cell lines under stress conditions, we performed targeted lipidomics on *MTARC1*-KO cells

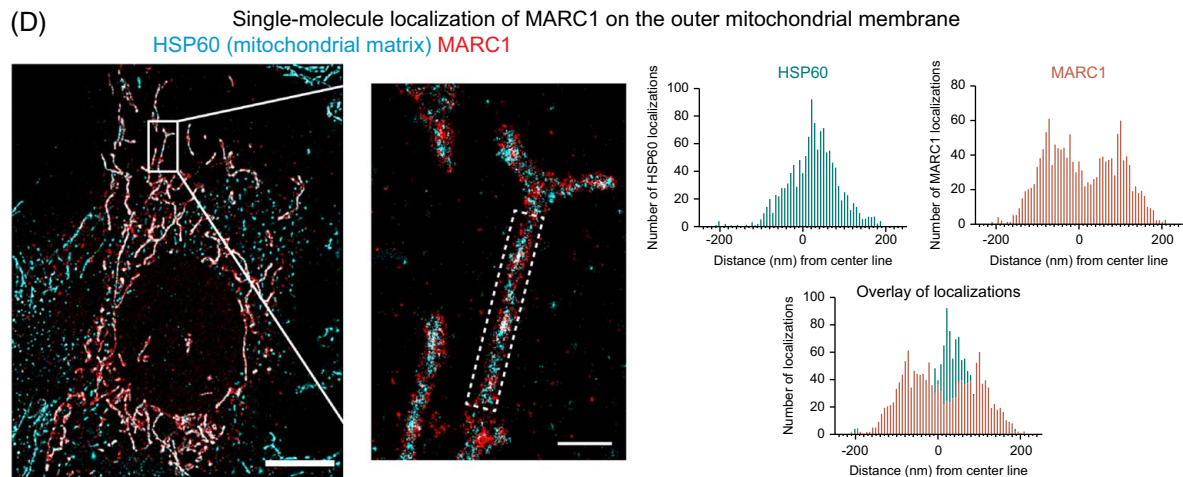
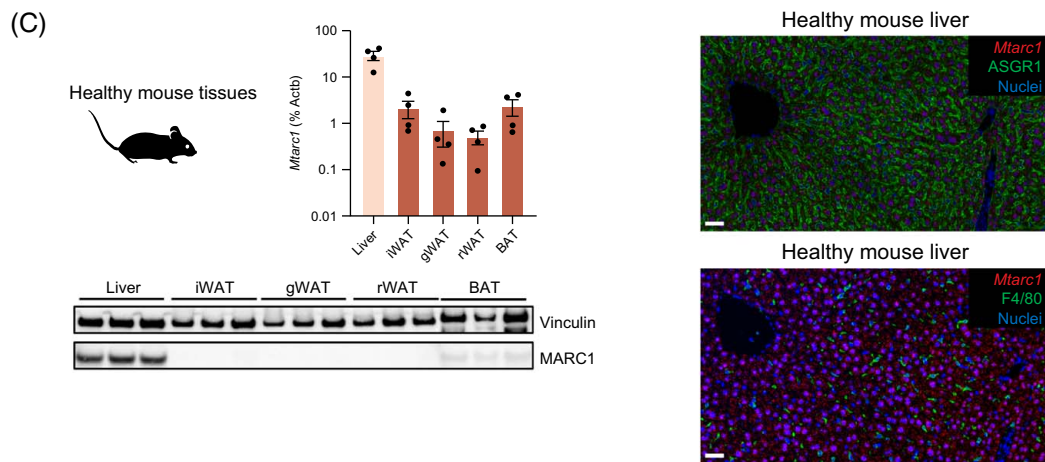
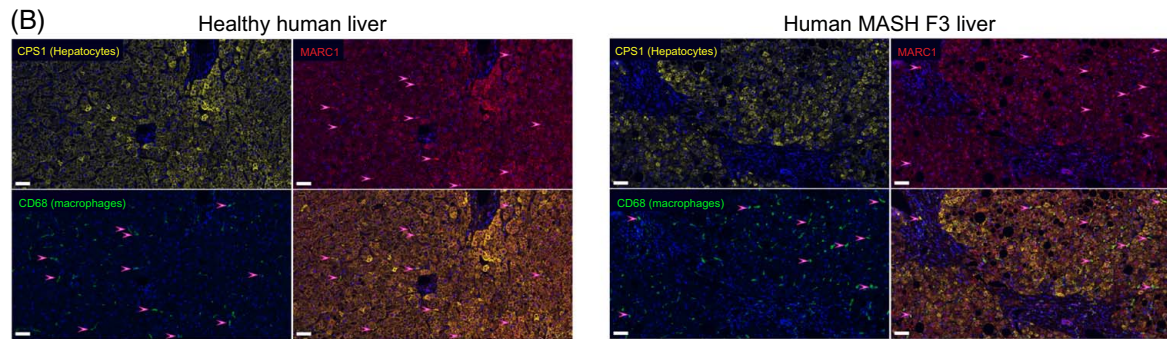
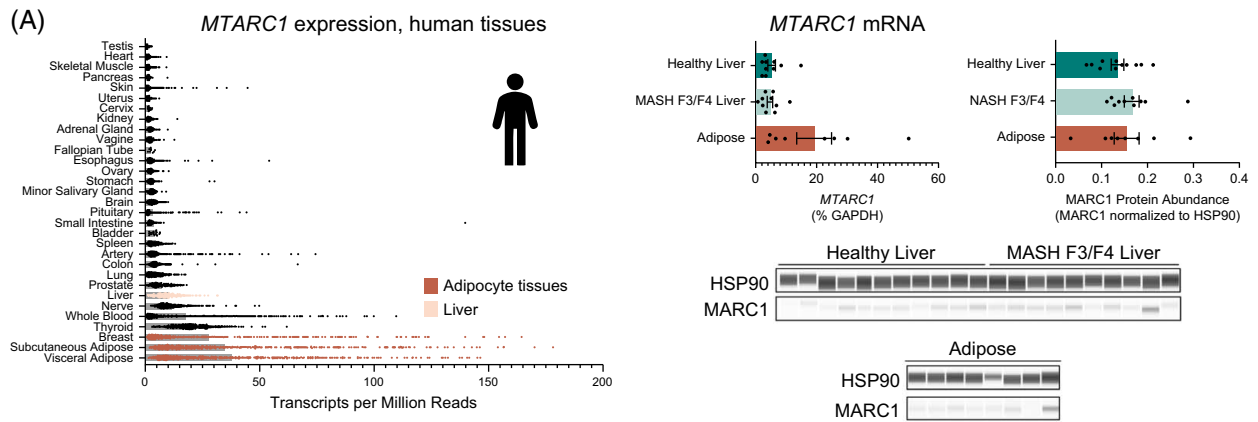


FIGURE 2 mARC1 expression profile differs in human and mouse tissues and mARC1 protein localizes to the outer mitochondrial membrane. (A) Human mARC1 expression from GTEx database (mRNA, TPM) and by qPCR and western blots in human liver and adipose tissue. (B) Immunofluorescence imaging of human healthy and MASH (fibrosis score 3) livers (nuclei = blue, carbamoyl phosphate synthetase [CPS1] hepatocytes = yellow, mARC1 = red, CD68 = green). Pink arrowheads highlight CD68/mARC1 coexpression. Scale bars, 50 μ m. (C) mARC1 RNA and protein expression in mouse liver, inguinal (iWAT), gonadal (gWAT), and perirenal (rWAT) white adipose tissue and brown adipose tissue (BAT). Multiplexed *Mtarc1* in situ hybridization (red) and immunofluorescence colocalization with ASGR1 (hepatocytes/green) or F4/80 (macrophages/green) and nuclei (blue) in mouse liver. Scale bars, 50 μ m. (D) Single-molecule localization of mARC1 (red) and heat shock protein 60 (HSP60 = mitochondrial matrix/blue) in cultured human cells. Scale bars, 10 μ m and 1 μ m (inset). n = 20 human liver and 8 human adipose samples in western blots and qPCR. Data in bar graphs are presented as mean \pm SEM with individual data points represented. Abbreviations: CD68, cluster of differentiation 68; GAPDH, glyceraldehyde-3-phosphate dehydrogenase; GTEx, genotype-tissue expression; mARC1, mitochondrial amidoxime-reducing component 1; MASH, metabolic dysfunction-associated steatohepatitis; qPCR, quantitative reverse transcription polymerase chain reaction; TPM, transcripts per million.

treated with palmitate, fructose, and insulin. In *MTARC1*-KO cells, there were reductions in Cholesteryl Ester 16:1, Ceramide d18:1/22:1, and triglyceride 46:3-fatty acid 16:1 (Figure 3F). Among the cholesteryl ester and triglyceride species, the most significant changes in abundance were observed in poly-unsaturated lipids (20:4, 22:5, or 22:6) (Supplemental Figure S3F, <http://links.lww.com/HC9/A803> and Supplemental Data Table S9, <http://links.lww.com/HC9/A799>).

Multiomics analysis of hepatocyte-specific *Mtarc1* knockdown in a lipotoxicity setting reveals modulation of specific lipid classes and hepatocyte-immune cross-talk

To build upon in vitro observations that mARC1 promotes steatosis and oxidative stress, we tested *Mtarc1* knockdown in an acute lipotoxicity setting by feeding mice the Gubra-amylin-NASH overnutrition diet for 6 weeks (Figure 4A). Target engagement was confirmed in hepatocytes by in situ hybridization showing the absence of cytoplasmic *Mtarc1* but leaving nascent nuclear mRNA (Supplemental Figure S4A, <http://links.lww.com/HC9/A804>). In bulk liver RNA, GalNAc-si*Mtarc1* achieved > 87% knockdown (Supplemental Figure S4B, <http://links.lww.com/HC9/A804>). GalNAc-si*Mtarc1* reduced weight gain (Figure 4B) and circulating concentrations of biomarkers consistent with human GWAS associations, including serum cholesterol, LDL, and HDL (Figure 4C). GalNAc-si*Mtarc1* reduced hepatic mitochondrial DNA, thiobarbituric acid reactive substances, and 8-iso-PGF2 α content, confirming the role of mARC1 in oxidative stress (Figure 4D). Total hepatic lipids trended ($p=0.07$) to reduce with GalNAc-si*Mtarc1*, with the greatest effect in cholesterol ester and triglyceride lipid classes (Figure 4E, Supplemental Data Table S10, <http://links.lww.com/HC9/A799>).

RNA sequencing was performed from the livers of GalNAc-si*Mtarc1*-treated mice (Figure 4F). *Mtarc1* knockdown modulated gene expression in the Gubra-amylin-NASH diet setting, and some differentially expressed genes were regulated by *Mtarc1*, independent of the dietary setting. These mARC1-dependent

differentially expressed genes were broadly involved in body weight regulation (*H19* [long noncoding RNA H19], *Ntrk2* [neurotrophic receptor tyrosine kinase 2]), cell cycle regulation (*Ccnd1Whm* [Cyclin D1 Whirlin], *Llrm2* [leucine-rich repeats and transmembrane domain 2], *Ly6d* [lymphocyte antigen 6 family member D], *Nap1l3* [nucleosome assembly protein 1 like 3]), other outer mitochondrial membrane proteins (*Maoa* [monoamine oxidase A]), and immune signaling (*Cxcl13* [chemokine CXC motif ligand 3], *Trem2* [triggering receptor expressed on myeloid cells 2], *Ly6d*) (Figure 4F, Supplemental Data Table S11, <http://links.lww.com/HC9/A799>). Pathway enrichment analysis of genes regulated by mARC1 during lipotoxicity identified innate immunity, immunity, and inflammatory response as pathways with overrepresentation (12.2, 14.2, 4.7%, respectively, Figure 4F). To validate the role of mARC1 in hepatocyte-immune crosstalk and rule out the possibility of a confounding immune response due to the GalNAc-siRNA modality, the 6-week lipotoxicity experiment was repeated in a second cohort of mice including a GalNAc-siControl. GalNAc-si*Mtarc1* did not change the total number of CD45-positive cells and no immune cell subpopulations were affected by GalNAc-siControl as measured by flow cytometry (Supplemental Figure S4C, <http://links.lww.com/HC9/A804>). GalNAc-si*Mtarc1* reduced the amount of CD4-positive T-helper cells compared with untreated mice (Figure 4F, Supplemental Figure S4C, <http://links.lww.com/HC9/A804>).

Hepatocyte-specific *Mtarc1* knockdown reduces body weight, hepatic lipid content, and markers of fibrogenesis

The therapeutic potential of mARC1 in MASH was tested using DIO-NASH mice available at Gubra that have preexisting NASH and are obese at the time of treatment.^[29,30] GalNAc-si*Mtarc1* (88% knockdown) induced ~8% body weight loss after 12 weeks, concurrent with a reduction in fat mass and no change in food intake (Figure 5A, Supplemental Figures S5A, S5B, <http://links.lww.com/HC9/A805>). Consistent with observations in the acute lipotoxicity setting, GalNAc-si*Mtarc1* reduced plasma cholesterol, LDL, and HDL in DIO-NASH mice (Supplemental Figure 5C, <http://links.lww.com/HC9/A805>).

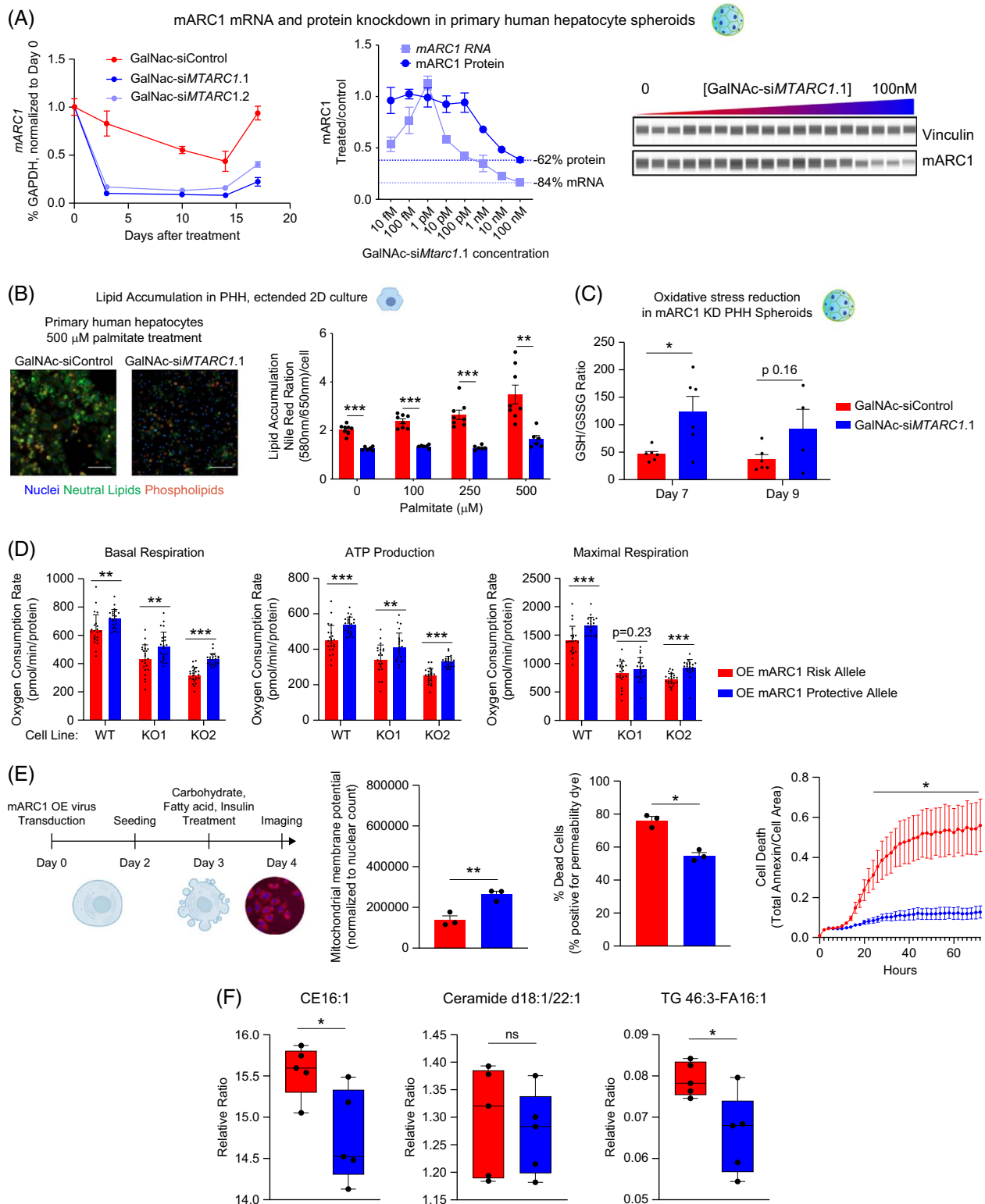


FIGURE 3 mARC1 expression modulation by genetic tools affects steatosis, oxidative stress, cell death, and lipid profile in human in vitro hepatocyte models. (A) Time course and dose-response of mARC1 RNA and protein in PHH spheroids treated with GalNac-siMTARC1. $n=2$ wells. (B) Lipid accumulation in the 2-dimensional culture of GalNac-siMTARC1.1-treated PHHs assessed by Nile Red fluorescence assay, nuclei (blue), neutral lipids (green), and phospholipids (yellow). Scale bars, 100 μm . $n=6-8$ /group. (C) Ratio of reduced to oxidized glutathione in PHH spheroids treated with GalNac-siMTARC1.1 at days 7 and 9 after treatment. $n=6$ /group. (D) Oxygen consumption rate parameters measured in mARC1 KO cell lines overexpressing mARC1 risk and protective (p.R200*) alleles. $N=24$ /well/group. (E) Quantification of mitochondrial membrane potential, cell permeability, and annexin V in palmitate, fructose, and glucose-treated mARC1 overexpressing cells measured by live-cell microscopy. $n=3$ /group. (F) Quantification of lipid species in mARC1 OE mARC1 KO cell lines. $n=5$ /group. Data are presented as mean \pm SEM. * $p \leq 0.05$, ** $p \leq 0.01$, *** $p \leq 0.001$, one-way ANOVA or t test. Abbreviations: GAPDH, glyceraldehyde-3-phosphate dehydrogenase; KO, knockout; mARC1, mitochondrial amidoxime-reducing component 1; OE, overexpression; PHH, primary human hepatocytes; WT, Wild-type.

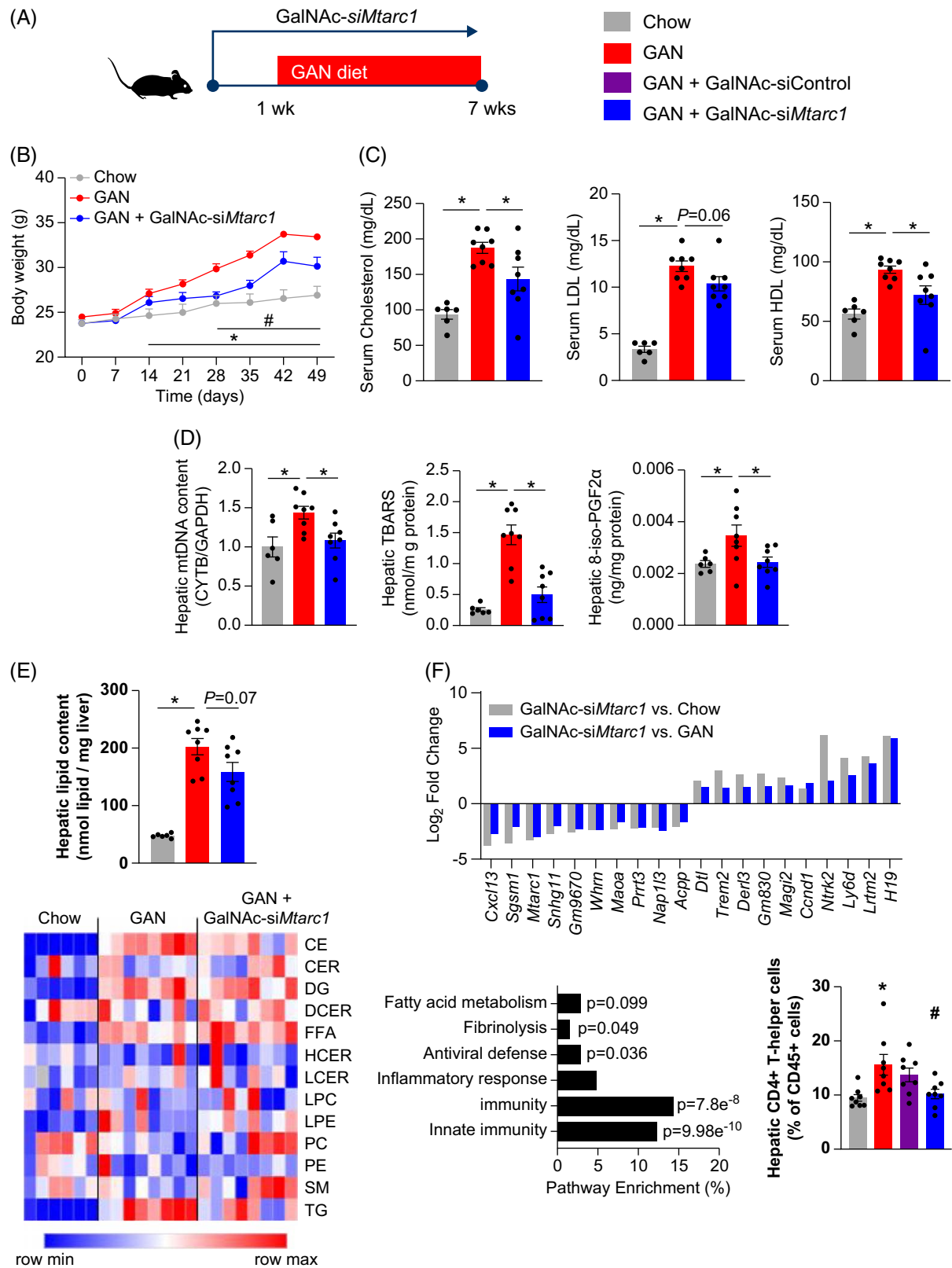


FIGURE 4 mARC1 depletion by GalNAc-siMtarc1 (3 mg/kg) reduces hepatic steatosis and oxidative stress in a lipotoxicity setting. (A) Experimental design (n=6–8 mice/group). (B) Body weight curve. (C) Serum cholesterol biomarkers. (C) Hepatic mitochondrial DNA content and oxidative stress markers. (E) Quantification of total hepatic lipid content and specific lipid classes. (F) DEGs by GalNAc-siMtarc1, pathway enrichment of DEG by GalNAc-siMtarc1 versus GAN, hepatic flow cytometry analysis. Data are presented as mean \pm SEM. Data sets with 3 groups: one-way ANOVA ($*p < 0.05$). Data sets with 4 groups: t test Chow versus GAN ($*p < 0.05$), then one-way ANOVA with Dunnett's test.

compare GalNAc-treatment to GAN ($\#p < 0.05$). Longitudinal data were analyzed by two-way ANOVA with repeated measures ($*p < 0.05$ GAN vs. chow, $\#p < 0.05$ GalNAc-si*Mtarc1* vs. GAN). Abbreviations: CYTB, Cytochrome B; DEG, differentially expressed gene; GAN, Gubra-amylin-NASH diet; GAPDH, glyceraldehyde-3-phosphate dehydrogenase; mARC1, mitochondrial amidoxime-reducing component 1; PGF2 α , prostaglandin F2alpha; TBARS, thiobarbituric acid reactive substances.

[lww.com/HC9/A805](http://links.lww.com/HC9/A805)). GalNAc-si*Mtarc1* improved liver injury biomarkers, including reductions in plasma cytokeratin 18-M65 (total cell death) and alanine aminotransferase concentrations (Figure 5B). In the liver, GalNAc-si*Mtarc1* reduced steatosis and oxidative stress marker 4-hydroxy-nonenal (Figure 5C). GalNAc-si*Mtarc1* reduced hepatic mRNA markers of fibrogenesis *Col1a1* (collagen type 1 alpha 1), *Col3a1* (collagen type 3 alpha 1), and *Timp1* but did not improve the Sirius red morphometry area (Figure 5D). There were no improvements in plasma cytokeratin 18-M30 (apoptosis) or hepatic terminal deoxynucleotidyl transferase dUTP nick end labeling and alpha smooth muscle actin area with GalNAc-si*Mtarc1* (Supplemental Figures S5C, S5D, <http://links.lww.com/HC9/A805>). To identify plasma-lipids correlating with liver mARC1 protein expression, we clustered all abundance correlation profiles by Pearson and zoomed into the plasma lipid module of interest (Figure 5E). This revealed a dependency of 18-carbon chain length ceramides and hexosylceramides in the plasma with liver mARC1 expression (Figure 5E). The reduction of plasma Ceramide d18:1/22:1, Cholesterol ester 16:1, Sphingomyelin 18:1/22:1, and Hexosylceramide d18:1/22:1 with GalNAc-si*Mtarc1* were confirmed by targeted lipidomics (Figure 5F, Supplemental Data Table S12, <http://links.lww.com/HC9/A799>).

Level of hepatocyte-specific *Mtarc1* knockdown correlates with specific lipid and protein species

A second study of a similar therapeutic design in DIO-NASH mice was performed using a GalNAc-si*Mtarc1* dose-response (Figure 6A, Supplemental Figure S6A, <http://links.lww.com/HC9/A806>). GalNAc-si*Mtarc1* reduced plasma cholesterol concentrations in a dose-dependent manner; however, the magnitude of reduction in plasma TIMP1 (metallopeptidase inhibitor 1), PIIINP (procollagen III N-terminal peptide), and cytokeratin 18-M65 concentrations was similar across dose groups (Figure 6B, Supplemental Figure S6B, <http://links.lww.com/HC9/A806>). GalNAc-si*Mtarc1* reduced hepatic steatosis but did not affect the alpha smooth muscle actin area, consistent with previous studies (Figure 6C, Supplemental Figures S6C, S6D, <http://links.lww.com/HC9/A806>). To validate the lipid biomarkers related to mARC1 hepatic abundance (Figure 5F) and further explore mechanisms related to mARC1 on the proteome level, we performed a targeted analysis of the plasma lipid candidates identified previously (Figure 5F) and unbiased proteomics from the

liver in this dose-dependent setting. We validated that the plasma abundance of Ceramide d18:1/22:1, Phosphatidyl Choline 16:0/18:1, and Sphingomyelin d18:1/22:1 was dose-dependently reduced in plasma by GalNAc-si*Mtarc1* (Figure 6D). We observed a high correlation ($R^2 = 0.60$) of plasma Ceramide 18:1/22:1 and liver mARC1 protein, rendering this lipid a promising liquid biomarker candidate (Figure 6E). Our liver proteomics revealed a correlation between the abundance of hepatic proteins related to mitochondrial function and lipid handling and transport with mARC1, including TMEM245 [transmembrane protein 245], ACAA1A, GPAM (glycerol 3 phosphate acyltransferase), ACAA1B, SLC25A17, CRAT (carnitine o-acetyltransferase), ACOT12 (acetyl-coenzyme A thioesterase 12), ASCL4 (long-chain-fatty-acid-CoA ligase 4), SLC25A20, and SLC25A10 ($R^2 = 0.69-0.31$; Figure 6F, Supplemental Data Table S13, <http://links.lww.com/HC9/A799>).

mARC1 modulates lipid accumulation in human adipocytes

We used siRNA compounds (si*MTARC1*) to knock down *MTARC1* in human primary stromal vascular fraction (SVF)-derived adipocytes. *MTARC1* is not expressed in the precursor SVF cells but increases in expression throughout the differentiation and maturation process (Supplemental Figure S7A, <http://links.lww.com/HC9/A807>). We tested SVF cells derived from visceral (omental) and subcutaneous adipose depots and observed low differentiation efficiency (data not shown) in the visceral SVF cells, concomitant with low *MTARC1* expression when compared with subcutaneous SVF-adipocytes. *MTARC1* expression increased 2000-fold throughout a 21-day culture time course of subcutaneous SVF-adipocytes, and 1000-fold during the first week of differentiation. Therefore, we differentiated the cells for 1 week, then treated them with si*MTARC1* during the second week of adipocyte maturation (Figure 7B). Two si*MTARC1* compounds of differing potency were used (XD38785 and XD38758, of intermediate and high potency, respectively) in SVF-adipocytes derived from 3 human donors.

On culture day 12 (5 days after siRNA treatment), the lipid droplet content of si*MTARC1*-treated adipocytes was visibly decreased when observed by fluorescent microscopy (Figure 7C). This qualitative microscopy-based assessment of lipid droplet accumulation was complemented by biochemical analyses of triglyceride content in the adipocytes. Triglyceride abundance was decreased in proportion to the amount of knockdown

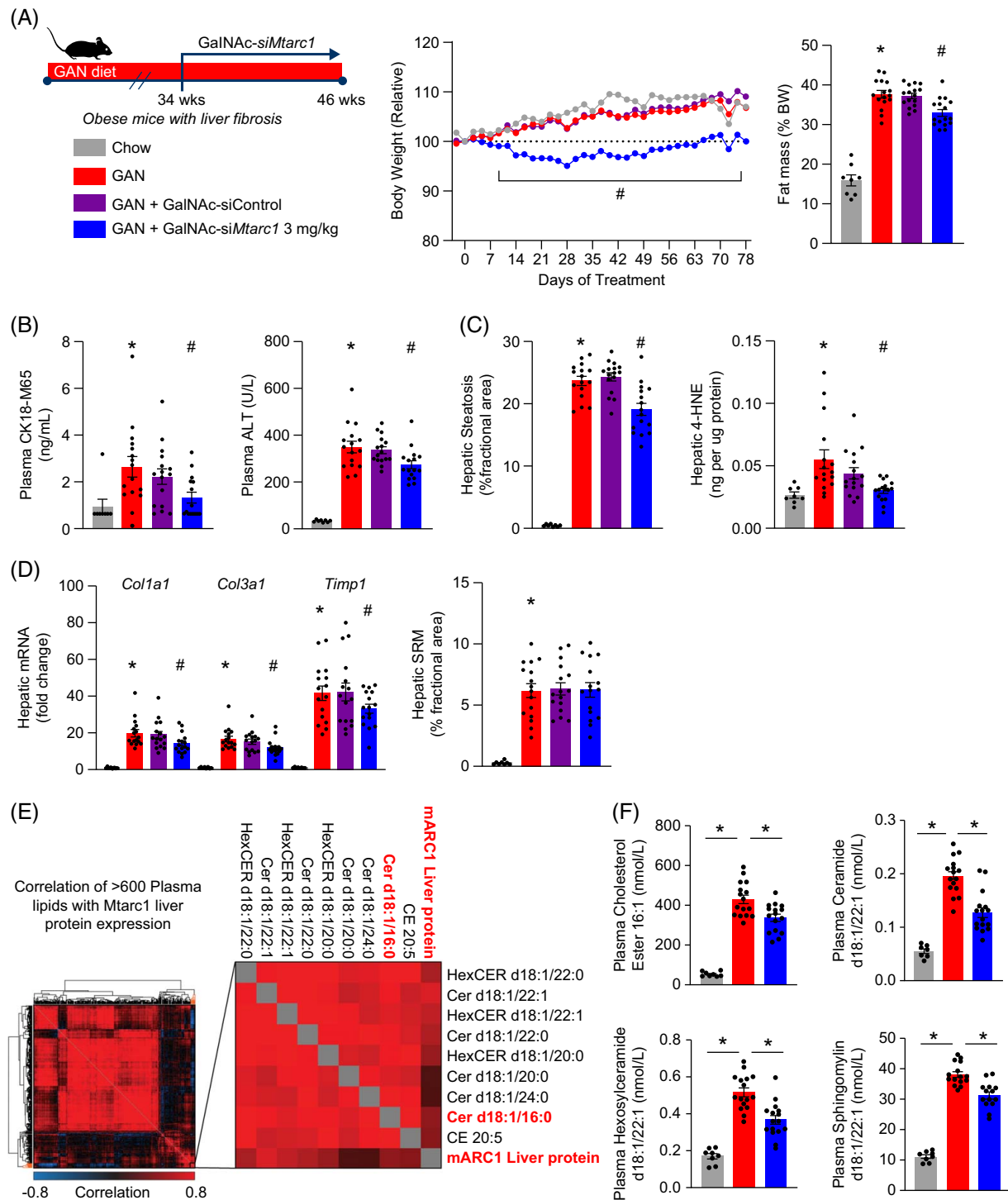


FIGURE 5 mARC1 depletion by GalNAc-siMtarc1 reduces steatosis, cell death, and fibrogenesis markers in a therapeutic MASH setting. (A) Experimental design (n=8–16 mice/group), relative body weight change, and body fat mass after 12 weeks GalNAc-siMtarc1. (B) Circulating biomarkers of hepatocyte health. (C) Quantification of hepatic steatosis and hepatic oxidative stress. (D) Hepatic fibrogenesis mRNA and fibrosis area. Circulating fibrogenesis biomarker, hepatic mRNA, and fibrosis area. (E) Left: Profiling of global plasma lipidomics correlation with Mtarc1 hepatic protein expression; Right: Zoomed-in cluster representing greatest Mtarc1 protein correlation to distinct lipids. (F) Selected plasma lipids correlating with Mtarc1 hepatic protein expression. Data are presented as mean \pm SEM. Data sets with 3 groups: one-way ANOVA ($*p < 0.05$). Data sets with 4 groups: *t* test Chow versus GAN ($*p < 0.05$), then one-way ANOVA with Dunnett's compared GalNAc-treatment to GAN ($\#p < 0.05$). Longitudinal data were analyzed by two-way ANOVA with repeated measures ($\#p < 0.05$ GalNAc-siMtarc1 vs. GAN). Abbreviations: 4-HNE, 4-hydroxy-nonal; ALT, alanine aminotransferase; BW, body weight; GAN, Gubra-amylin-NASH diet; mARC1, mitochondrial amidoxime-reducing component 1; MASH, metabolic dysfunction-associated steatohepatitis; SRM, Sirius red morphometry.

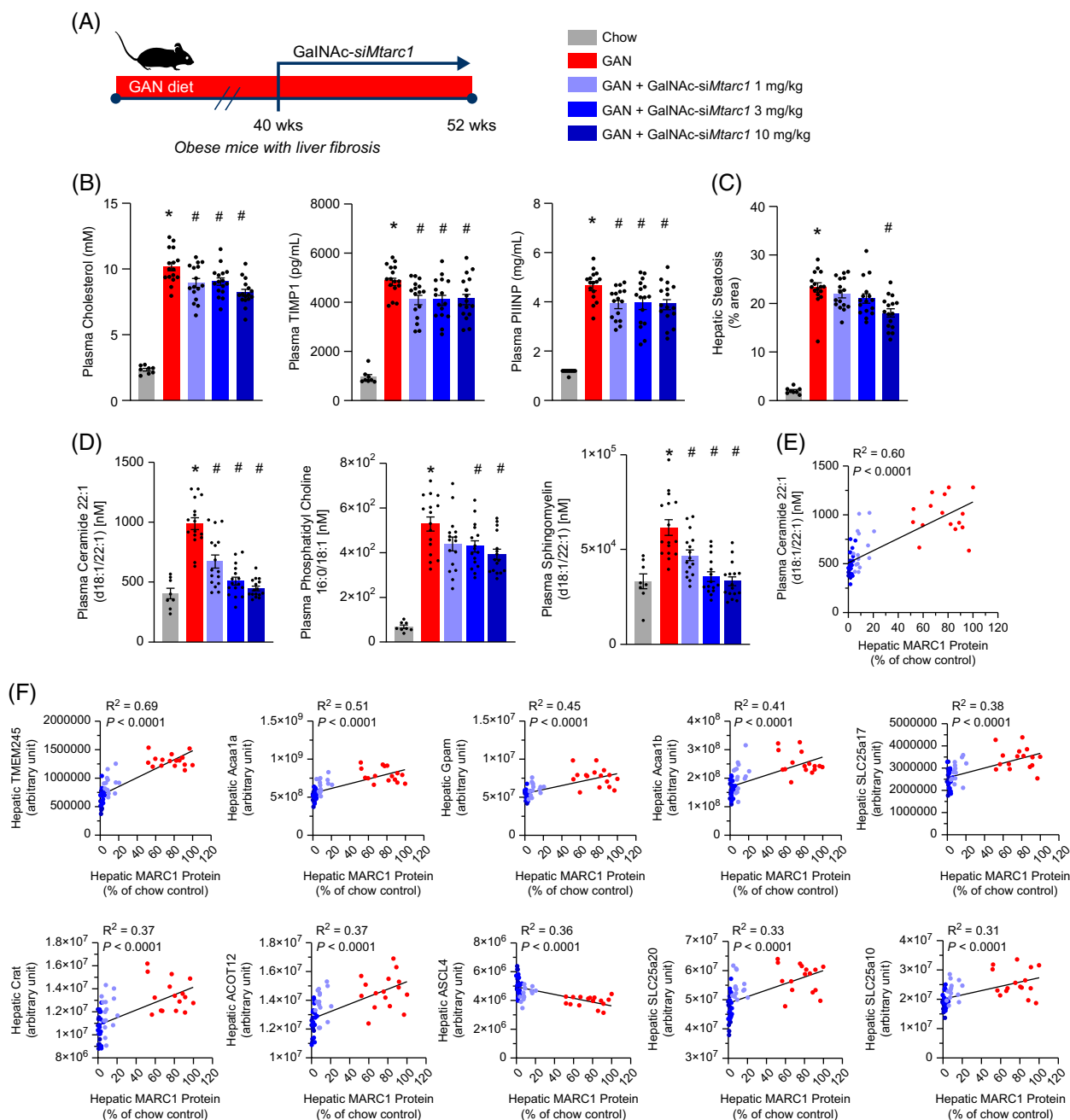


FIGURE 6 Dose-responsive effects of GalNac-siMtar1 on lipidomic and proteomic profile in a therapeutic MASH setting. (A) Experimental design ($n = 8\text{--}16$ mice/group). (B) Serum cholesterol and fibrogenesis biomarkers. (C) Quantification of hepatic steatosis. (D) Plasma abundance of targeted lipid species. (E) Correlation of plasma Ceramide d18:1/22:1 with hepatic mARC1 protein. (F) Correlation of hepatic proteins and mARC1 expression. Data are presented as mean \pm SEM. Data were analyzed by t test to compare control and diet conditions ($*p < 0.05$), then a one-way ANOVA with Dunnett's to compare GalNac-treated groups to diet ($\#p < 0.05$). Correlations were generated by linear regression. Abbreviations: ACOT12, acetyl-coenzyme A thioesterase 12; ASCL4, long-chain-fatty-acid-CoA ligase 4; GAN, Gubra-amylin-NASH diet; mTARC1, mitochondrial amidoxime-reducing component 1; MASH, metabolic dysfunction-associated steatohepatitis; PIIINP, procollagen III N-terminal peptide; SLC25a17, solute carrier family 25 member 17; TIMP1, metalloproteinase inhibitor 1.

achieved with each siMtar1 (Figure 7D). The more potent siMtar1 yielded a 51%–65% reduction in triglycerides, and the less potent siMtar1 yielded a 16%–39% reduction in triglycerides (Figure 7D). Triglyceride lipolysis was increased in mARC1-depleted adipocytes under basal serum starvation conditions in adipocytes from 2 different human

donors, but no consistent difference in activated lipolysis was observed (Supplemental Figure S7B, <http://links.lww.com/HC9/A807>). We hypothesized that this increase in basal lipolysis would result in increased oxygen consumption because of increased fatty acid oxidation; however, we observed no difference in oxygen consumption rate in the adipocytes assayed

after si*MTARC1* treatment (representative data in Supplemental Figure S7C, <http://links.lww.com/HC9/A807>). si*MTARC1* treatment also did not affect the percentage of cells that differentiated into adipocytes (Supplemental Figure S7D, <http://links.lww.com/HC9/A807>).

Our observation that si*MTARC1* reduced triglycerides in adipocytes was supported by targeted lipidomics performed on SVF-adipocytes derived from one donor. The lipidomics analyses revealed reductions in intracellular C16 and C16:1-containing species in all measured lipid classes in si*MTARC1*-treated adipocytes (Supplemental Figure S7F, <http://links.lww.com/HC9/A807>), including several species that also were affected by mARC1 modulation in the in vitro hepatocyte and in vivo MASH models (Figure 7E). As observed in hepatocytes (Supplemental Figure S3F, <http://links.lww.com/HC9/A803>), the specific lipid species increased after *MTARC1* knockdown incorporated highly unsaturated fatty acids (Supplemental Figure S7E, <http://links.lww.com/HC9/A807>, Supplemental Data Table S14, <http://links.lww.com/HC9/A799>).

We developed the hypothesis that in vivo in humans, *MTARC1* knockdown may reduce the abundance of systemic factors derived from adipocytes that promote MASH. To test this hypothesis, we performed RNA profiling using a metabolism-focused multiplexed RNA hybridization array (Supplemental Figure S7F, S7G, <http://links.lww.com/HC9/A807>, Supplemental Data Table S15, <http://links.lww.com/HC9/A799>) and profiled secreted proteins (Supplemental Figure S7H, <http://links.lww.com/HC9/A807>, Supplemental Data Table S16, <http://links.lww.com/HC9/A799>) in the SVF-adipocytes treated with si*MTARC1*. Pathway enrichment analysis indicated that mitochondrial electron transport (eg, *COX8A* and *NDUFB8*) and apoptosis and cell stress pathways (eg, *GPX4*) were downregulated by *MTARC1* knockdown. The de novo lipogenesis genes *ACACA* and *ACACB* were decreased, while *CPT1A* was increased. mRNA and secreted protein for many proinflammatory factors were increased, including chemokine (C-C motif) ligands 4, 5, and 13 (*CCL4*, *CCL5*, and *CCL13*), and indoleamine 2,3 dioxygenase 1 (*IDO1*) (Supplemental Figures S7F, S7G, S7H, <http://links.lww.com/HC9/A807>).^[25] The abundance of the adipokines adiponectin (*ADIPOQ*), fatty acid binding protein 4 (*FABP4*), and leptin (*LEP*) in the media were not significantly altered, and PCSK9, PLTP, and SORT1 secretion were decreased by *MTARC1* knockdown (Figure 7F).

DISCUSSION

The goal of our work was to expand on the published genetic data linking mARC1 to human disease and to observe the molecular effects of mARC1 modulation in

preclinical MASH models. We observed that the protective *MTARC1* variants identified by genetics reduce mARC1 protein abundance and thus we propose that protein depletion would be an appropriate approach to model the genetic variants for therapeutic targeting of this protein. This contrasts with the data reported in Hudert et al^[31] where the *MTARC1* protective variant rs2643248 was not correlated with any change in hepatic mARC1 protein. We describe the reproducible benefits of mARC1 depletion on steatosis and cell death across both in vitro human hepatocytes and adipocytes, and in vivo MASH models, with specific lipid species modulated by mARC1 across these experimental systems (summarized in Figure 8). Our findings build upon the previously described role of mARC1 in N-reductive metabolism and add to a growing body of literature surrounding mARC1 in MASH^[15] by describing a functional role in adipocytes. We conclude that targeting hepatocyte mARC1 using GalNAc-siRNAs may improve dysmetabolism and steatosis outcomes to slow fibrogenesis in patients with MASLD.

We observed mARC1 effects in body weight regulation. GalNAc-si*Mtarc1* prevented body weight gain, induced body weight loss of obese mice, and upregulated H19 in mouse liver, a lincRNA inversely correlated with body mass index in humans.^[32] mARC1-targeted therapies might reduce body weight in humans, offering an added benefit to patients with MASLD who are typically of high body mass index.^[33] Consistent with these preclinical observations, the protective effects of *MTARC1* loss-of-function variants on MASH risk are amplified in patients with high body mass index in large-scale GWAS, although this has also been observed for other fatty-liver SNPs.^[8] These human genetic findings encouraged us to study mARC1 in human adipocytes, and we report human primary adipocyte phenotypes that are proportional to *MTARC1* knockdown, lending support for a direct role of mARC1 in adipose tissue lipid accumulation.

Cumulative evidence from our work and others^[15] implies a central role of mARC1 in lipid handling (Figure 8). From these data, we hypothesize that mARC1's role in lipid handling may be related to lipid synthesis, desaturation, or conjugation rather than fatty acid oxidation. Given that palmitate-containing species (16:0) are lipotoxic,^[34] their reduction by way of *MTARC1* knockdown would decrease lipid-driven oxidative stress, ER stress, and apoptosis signaling, consistent with our observations in preclinical MASH models. Whether the role of mARC1 in lipid handling is connected to N-reductive metabolism or is an independent molecular function of the protein remains unclear.

Subcellular localization, lipid trafficking, and protein-protein interactions may be areas of interest for future mARC1-focused studies. The genetic underpinnings of MASLD are centralized around the formation and

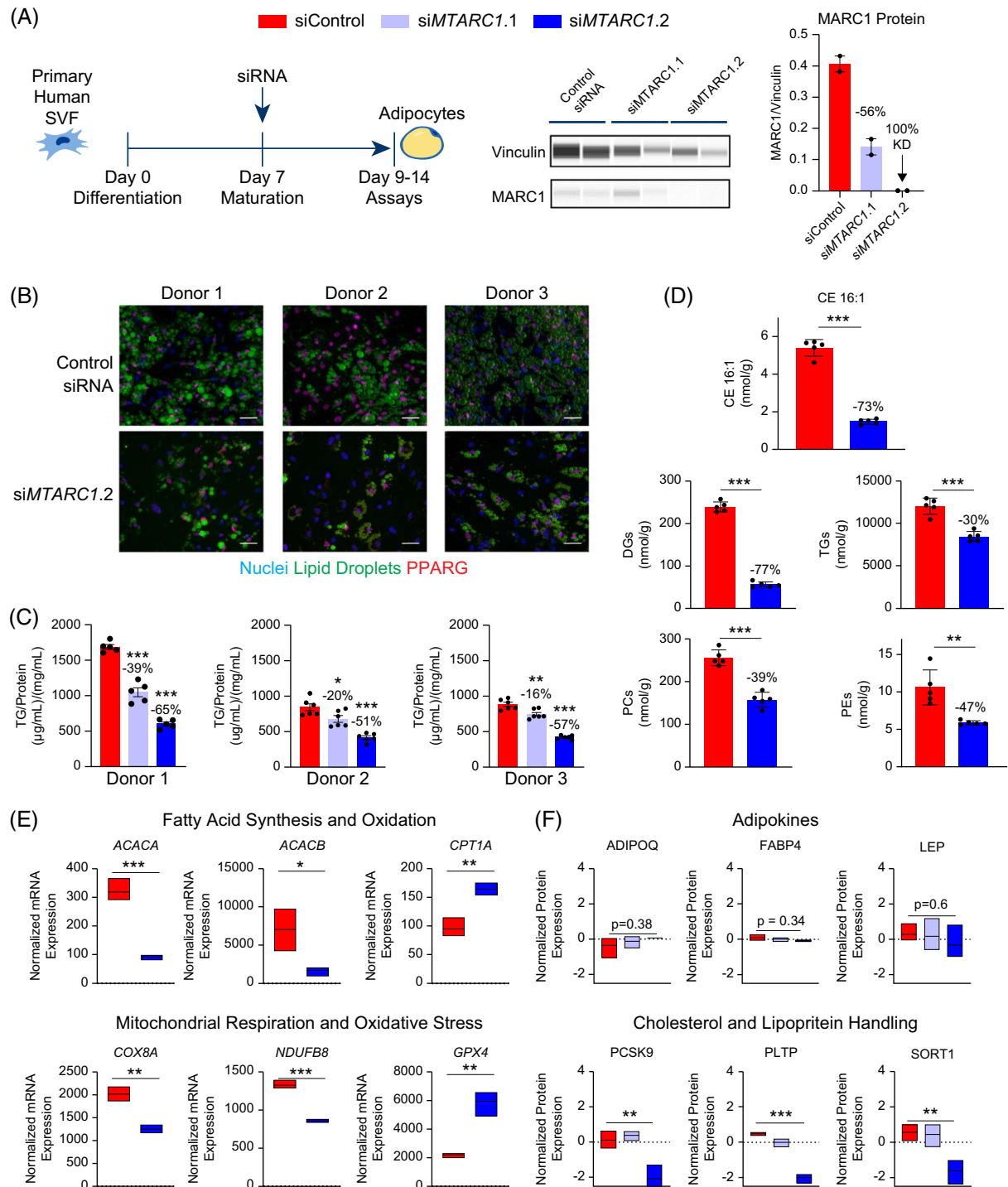


FIGURE 7 siMTARC1 treatment reduces triglyceride accumulation and cell death in human primary SVF-adipocytes. (A) Study plan for siMTARC1 treatment in primary human SVF-adipocytes and mARC1 knockdown percentage measured by western blot. $n = 2$ wells. (B) Immunofluorescence imaging of nuclei (blue), lipid droplets (green), and PPARG (red). (C) Biochemical quantitation of TG abundance in siMTARC1.2-treated primary human SVF-adipocytes from 3 human donors. Scale bar = 100 μm . $n = 5$ wells/group. (D) LC/MS quantitation of cholesteryl ester 16:1, and lipid classes in siMTARC1.2-treated primary human SVF-adipocytes from one human donor. $n = 5$ samples per group. (E) RNA and (F) secreted protein abundance of adipokines in siMTARC1-treated primary human SVF-adipocytes from 3 human donors. $n = 3$ for RNA, $n = 5$ for protein. Data in bar graphs presented as mean \pm SEM. $*p \leq 0.05$, $**p \leq 0.01$, $***p \leq 0.001$, one-way ANOVA or t test. Abbreviations: LC/MS, Liquid chromatography/Mass spectrometry; mTARC1, mitochondrial amidoxime-reducing component 1; PPARG, Peroxisome proliferator activated receptor gamma; SVF, stromal vascular fraction of adipose tissue.

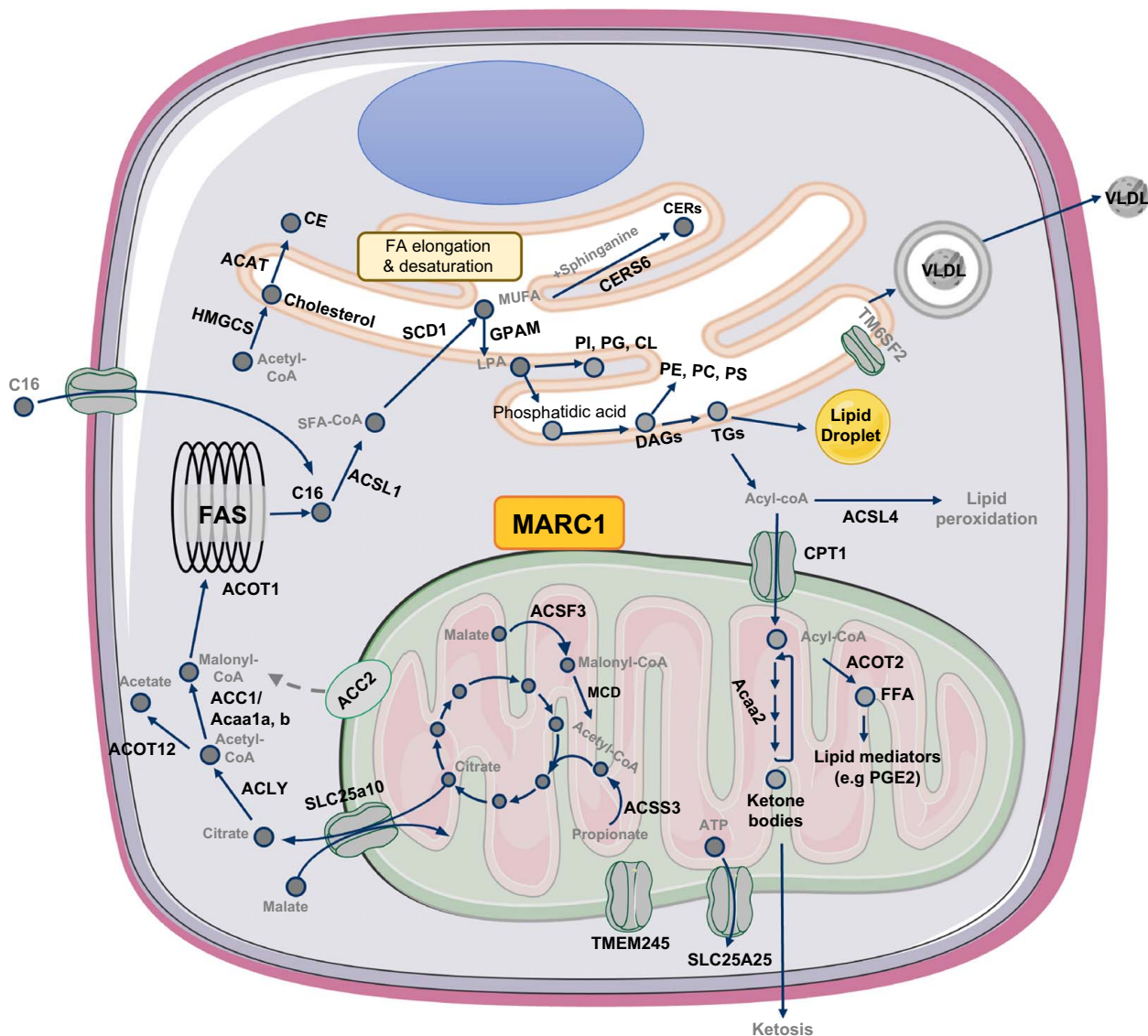


FIGURE 8 Schematic summary of molecular profiling observations in mARC1 preclinical models and relationship to known MASH-relevant metabolic pathways. Specific factors modulated by mARC1 are in black font. Abbreviations: ACOT12, acetyl-coenzyme A thioesterase 12; mARC1, mitochondrial amidoxime-reducing component 1; MASH, metabolic dysfunction-associated steatohepatitis; TMEM245, transmembrane protein 245.

trafficking of lipid droplets between organelles.^[35,36] With its positioning on the outer mitochondrial membrane, mARC1 has the potential to interact with proteins on neighboring organelles and thereby influence lipid synthesis and trafficking pathways. For example, mARC1 interacts with transmembrane 6 superfamily member 2 (TM6SF2), an ER-Golgi membrane protein involved in lipidation of very low-density lipoproteins.^[37] It is not yet clear what function the mARC1-TM6SF2 interaction serves.

We raise the possibility that mARC1 has a role in immune cells. This inflammatory role may be direct, as mARC1 protein was observed in human hepatic CD68+ (macrophage) cells. However, our ability to test mARC1's mechanism in macrophages was hindered by the lack of sustained mARC1 expression in primary

cells in vitro. In addition, the inflammatory role of mARC1 may be indirect, as we observed the hepatocyte-immune crosstalk in vivo after hepatocyte knock-down, and in human adipocytes mARC1 depletion promoted proinflammatory protein secretion. The directionality, implications, and tissue-specific effects of mARC1 in inflammation will be an area of further investigation.

In conclusion, our phenotyping data can be used for generating hypotheses about the disease-relevant function of mARC1, but further mechanistic experiments are required to delineate the precise molecular function of mARC1 in disease. In addition, specific lipid species identified may be considered as biomarkers of mARC1 for application in future clinical studies. These insights will benefit translational strategies and mechanistic

understanding to strengthen the potential for mARC1 therapy in patients with MASLD or MASH.

ACKNOWLEDGMENTS

The authors appreciate H. Qian, J. Jeon, and M. Dugas from Boehringer Ingelheim for their technical assay expertise and contributions. The authors also thank the teams at Gubra A/S for performing studies in the biopsy-confirmed DIO-NASH mouse model and at Axolabs GmbH for screening and synthesis of GalNAc-siRNA compounds. Much of the *in silico* research in this paper has been conducted using the UK Biobank, a major biomedical database (www.ukbiobank.ac.uk). They also want to acknowledge the participants and investigators of the FinnGen study. The graphical abstract was prepared using Biorender.

FUNDING INFORMATION


This work was supported by Boehringer Ingelheim Pharmaceuticals, Ridgefield, CT, USA, and Boehringer Ingelheim Pharma GmbH & Co, Biberach an der Riss, Germany.

CONFLICTS OF INTEREST

All authors are presently employed by or have received research funding from Boehringer Ingelheim. Dmitriy Drichel consults for Boehringer Ingelheim and Merck. Martin Giera owns stock in Gilead and GlaxoSmithKline.

ORCID

Besnik Bajrami  <https://orcid.org/0000-0002-3827-8150>

Abdullah Mesut Erzurumluoglu  <https://orcid.org/0000-0003-1322-8138>

Curtis R. Warren  <https://orcid.org/0009-0004-7019-758X>

REFERENCES

- Rinella ME, Lazarus JV, Ratziu V, Francque SM, Sanyal AJ, Kanwal F, et al. A multi-society Delphi consensus statement on new fatty liver disease nomenclature. *J Hepatol.* 2023;78:1966–86.
- Sanyal AJ, Harrison SA, Ratziu V, Abdelmalek MF, Diehl AM, Caldwell S, et al. The natural history of advanced fibrosis due to nonalcoholic steatohepatitis: Data from the simtuzumab trials. *Hepatology.* 2019;70:1913–27.
- Younossi ZM, Wong G, Anstee QM, Henry L. The global burden of liver disease. *Clin Gastroenterol Hepatol.* 2023;21:1978–91.
- Alkhoury N, Gornicka A, Berk MP, Thapaliya S, Dixon LJ, Kashyap S, et al. Adipocyte apoptosis, a link between obesity, insulin resistance, and hepatic steatosis. *J Biol Chem.* 2010;285:3428–38.
- Plessis J du, Pelt J van, Korf H, Mathieu C, Schueren B van der, Lannoo M, et al. Association of adipose tissue inflammation with histologic severity of nonalcoholic fatty liver disease. *Gastroenterology.* 2015;149:635–648.e14.
- Tordjman J, Divoux A, Prifti E, Poitou C, Pelloux V, Hugol D, et al. Structural and inflammatory heterogeneity in subcutaneous adipose tissue: Relation with liver histopathology in morbid obesity. *J Hepatol.* 2012;56:1152–8.
- Munukka E, Pekkala S, Wiklund P, Rasool O, Borra R, Kong L, et al. Gut-adipose tissue axis in hepatic fat accumulation in humans. *J Hepatol.* 2014;61:132–8.
- Gao C, Marcketta A, Backman JD, O'Dushlaine C, Staples J, Ferreira MAR, et al. Genome-wide association analysis of serum alanine and aspartate aminotransferase, and the modifying effects of BMI in 388k European individuals. *Genet Epidemiology.* 2021;45:664–81.
- Kalinowski P, Smyk W, Nowosad M, Paluszkiwicz R, Michałowski Ł, Ziarkiewicz-Wróblewska B, et al. MTARC1 and HSD17B13 variants have protective effects on non-alcoholic fatty liver disease in patients undergoing bariatric surgery. *Int J Mol Sci.* 2022;23:15825.
- Sveinbjornsson G, Ulfarsson MO, Thorolfsson RB, Jonsson BA, Einarsson E, Gunnlaugsson G, et al. Multiomics study of nonalcoholic fatty liver disease. *Nat Genet.* 2022;54:1652–63.
- Erdin CA, Haas ME, Khara AV, Aragam K, Chaffin M, Klarin D, et al. A missense variant in Mitochondrial Amidoxime Reducing Component 1 gene and protection against liver disease. *PLoS Genet.* 2020;16:e1008629.
- Janik MK, Smyk W, Kruk B, Szczepankiewicz B, Górnicka B, Lebidzińska-Arciszewska M, et al. MARC1 p.A165T variant is associated with decreased markers of liver injury and enhanced antioxidant capacity in autoimmune hepatitis. *Sci Rep.* 2021;11:24407.
- Speliotes EK, Yerges-Armstrong LM, Wu J, Hernaez R, Kim LJ, Palmer CD, et al. Genome-wide association analysis identifies variants associated with nonalcoholic fatty liver disease that have distinct effects on metabolic traits. *PLoS Genet.* 2011;7:e1001324.
- Clement B, Struwe MA. The history of mARC. *Molecules.* 2023;28:4713.
- Lewis LC, Chen L, Hameed LS, Kitchen RR, Maroteau C, Nagarajan SR, et al. Hepatocyte mARC1 promotes fatty liver disease. *JHEP Rep.* 2023;5:100693.
- PercieduSert N, Hurst V, Ahluwalia A, Alam S, Avey MT, Baker M, et al. The ARRIVE guidelines 2.0: Updated guidelines for reporting animal research. *Exp Physiol.* 2020;105:1459–66.
- Allen AM, Therneau TM, Ahmed OT, Gidener T, Mara KC, Larson JJ, et al. Clinical course of non-alcoholic fatty liver disease and the implications for clinical trial design. *J Hepatol.* 2022;77:1237–45.
- Ott G, Reichmann D, Boerger C, Cascorbi I, Bittner F, Mendel R-R, et al. Functional characterization of protein variants encoded by nonsynonymous single nucleotide polymorphisms in MARC1 and MARC2 in healthy Caucasians. *Drug Metab Dispos.* 2014;42:718–25.
- Struwe MA, Clement B, Scheidig AJ. Letter to the editor: The clinically relevant MTARC1 p.Ala165Thr variant impacts neither the fold nor active site architecture of the human mARC1 protein. 2022;6:3277–8.
- Ott G, Havemeyer A, Clement B. The mammalian molybdenum enzymes of mARC. *JBIC J Biol Inorg Chem.* 2015;20:265–75.
- Aden DP, Fogel A, Plotkin S, Damjanov I, Knowles BB. Controlled synthesis of HBsAg in a differentiated human liver carcinoma-derived cell line. *Nature.* 1979;282:615–6.
- DuBridge RB, Tang P, Hsia HC, Leong PM, Miller JH, Calos MP. Analysis of mutation in human cells by using an Epstein-Barr virus shuttle system. *Mol Cell Biol.* 1987;7:379–87.
- PONTÉN J, MACINTYRE EH. Long term culture of normal and neoplastic human glia. *Acta Pathol Microbiol Scand.* 1968;74:465–86.
- SIEGEL MR, SISLER HD. Inhibition of protein synthesis *in vitro* by cycloheximide. *Nature.* 1963;200:675–6.
- Wakefield J. A Bayesian measure of the probability of false discovery in genetic epidemiology studies. *Am J Hum Genetics.* 2007;81:208–27.
- Carithers LJ, Moore HM. The Genotype-Tissue Expression (GTEx) Project. *Biopreserv Biobank.* 2015;13:307–8.

27. Ramachandran P, Dobie R, Wilson-Kanamori JR, Dora EF, Henderson BEP, Luu NT, et al. Resolving the fibrotic niche of human liver cirrhosis at single-cell level. *Nature*. 2019;575:512–8.
28. Klein JM, Busch JD, Potting C, Baker MJ, Langer T, Schwarz G. The Mitochondrial Amidoxime-reducing Component (mARC1) is a novel signal-anchored protein of the outer mitochondrial membrane. *J Biol Chem*. 2012;287:42795–803.
29. Hansen HH, Ægidius HM, Oró D, Evers SS, Heebøll S, Eriksen PL, et al. Human translatability of the GAN diet-induced obese mouse model of non-alcoholic steatohepatitis. *BMC Gastroenterol*. 2020;20:210.
30. Boland ML, Oró D, Tølbøl KS, Thrane ST, Nielsen JC, Cohen TS, et al. Towards a standard diet-induced and biopsy-confirmed mouse model of non-alcoholic steatohepatitis: Impact of dietary fat source. *World J Gastroenterol*. 2019;25:4904–20.
31. Hudert CA, Alisi A, Anstee QM, Crudele A, Draijer LG, Furse S, et al. Variants in MARC1 and HSD17B13 reduce severity of NAFLD in children, perturb phospholipid metabolism, and suppress fibrotic pathways. *Medrxiv*. 2020;2020.06.05.20120956.
32. Schmidt E, Dhaouadi I, Gaziano I, Oliverio M, Klemm P, Awazawa M, et al. LincRNA H19 protects from dietary obesity by constraining expression of monoallelic genes in brown fat. *Nat Commun*. 2018;3622:3622.
33. Wanless IR, Lentz JS. Fatty liver hepatitis (steatohepatitis) and obesity: An autopsy study with analysis of risk factors. *Hepatology (Baltimore, Md)*. 1990;12:1106–10.
34. Hirsova P, Ibrabim SH, Gores GJ, Malhi H. Lipotoxic lethal and sublethal stress signaling in hepatocytes: Relevance to NASH pathogenesis[S]. *J Lipid Res*. 2016;57:1758–70.
35. Trépo E, Valenti L. Update on NAFLD genetics: From new variants to the clinic. *J Hepatol*. 2020;72:1196–209.
36. Luukkonen PK, Qadri S, Ahlholm N, Porthan K, Männistö V, Sammalkorpi H, et al. Distinct contributions of metabolic dysfunction and genetic risk factors in the pathogenesis of non-alcoholic fatty liver disease. *J Hepatol*. 2022;76:526–35.
37. Luo F, Smagris E, Martin SA, Vale G, McDonald JG, Fletcher JA, et al. Hepatic TM6SF2 is required for lipidation of VLDL in a pre-Golgi compartment in mice and rats. *Cell Mol Gastroenterol Hepatol*. 2022;13:879–99.
38. Kurki MI, Karjalainen J, Palta P, Sipilä TP, Kristiansson K, Donner KM, et al. FinnGen provides genetic insights from a well-phenotyped isolated population. *Nature*. 2023;613:508–18.

How to cite this article: Jones AK, Bajrami B, Campbell MK, Erzurumluoglu AM, Guo Q, Chen H, et al. Mitochondrial amidoxime-reducing component 1 in metabolic dysfunction-associated steatotic liver disease: Modulation of lipid accumulation in human hepatocytes and adipocytes. *Hepatology Commun*. 2024;8:e0365. <https://doi.org/10.1097/HC9.0000000000000365>